sustainability

MDPI

Article

Microscopic Damage to Limestone under Acidic Conditions: Phenomena and Mechanisms

Xingming Chen [1], Xiaoping Liu [1], Haoming Luo [1], Linjian Long [1] and Chuanju Liu [1,2,*]

[1] School of Environment and Resources, Southwest University of Science and Technology, Mianyang 621010, China
[2] Shock and Vibration of Engineering Materials and Structures Key Laboratory of Sichuan Province, Southwest University of Science and Technology, Mianyang 621010, China
* Correspondence: liuchuanjuu@163.com

Abstract: In an acidic environment, the mineral components in rock begin to break down. As a result, the microstructure will be damaged, and then the mechanical properties will deteriorate, which will eventually have a negative effect on engineering stability. In order to study acid damage's effect on this kind of rock, limestone samples were acidified for 0 days, 5 days, 10 days, 15 days, and 20 days. The microstructure changes in the limestone after acidification were studied via the wave velocity test and electron microscope scanning, and the damage deterioration mechanism was revealed. The results show that the acoustic signal of acidified samples has an obvious absorption effect at high frequency, and the surface pore structure of acidified samples shows fractal characteristics. The P-wave velocity, main peak amplitude, and fractal dimension of the acidified samples did not gradually decrease with time; however, there was a short-term strengthening phenomenon during immersion, which was mainly caused by the formation of $CaSO_4$ crystals.

Keywords: acidic conditions; acoustic frequency domain; SEM; fractal dimension; microscopic damage

Citation: Chen, X.; Liu, X.; Luo, H.; Long, L.; Liu, C. Microscopic Damage to Limestone under Acidic Conditions: Phenomena and Mechanisms. *Sustainability* **2022**, *14*, 11771. https://doi.org/10.3390/su141811771

Academic Editor: Kaihui Li

Received: 27 July 2022
Accepted: 16 September 2022
Published: 19 September 2022

1. Introduction

Rocks and water have various chemical interactions that affect the strength and deformation characteristics of those rocks. Scholars have paid extensive attention to this phenomenon and achieved various results [1–3]. In addition, water in nature is often not of completely neutral pH but shows certain acidity or alkalinity. The continuous erosion in an acidic environment will change the basic surface structure of the rock, forcing the decomposition of mineral components within it, causing damage to the rock's microstructure, and then degrading the mechanical properties of the rock, posing a potential threat to the stability of rock-based civil engineering.

Li et al. [4] soaked sandstone in an acid solution and studied the microstructure and mechanical behavior of the sample after acidification. The microstructure shows that the reaction between the acid solution and sandstone minerals increases the number of pores and the dynamic strength of the sample decreases. Tong et al. [5] acidified granite and studied the microstructure changes of granite after acidification by SEM and NMR. It was found that the internal structure of the sample was damaged after acidification, and the degree of damage increased with the increase in the concentration of the solution. Morsy et al. [6] put shale from different areas in different concentrations of hydrochloric acid solution. The mass loss, composition analysis, and mineral assemblage characterization of samples after acid treatment were analyzed. It was found that the porosity of the samples after acid treatment increased, and the cracks and crack development in the samples after acid treatment were revealed. Feng et al. [7] soaked granite in an acid solution, studied the microdamage of granite after acidification, established the constitutive relationship among the damage variables, and studied the erosion effect of an acid solution on the mechanical degradation characteristics of granite. Yu et al. [8] carried out experimental research on

limestone eroded by an acidic solution, and analyzed the change characteristics of limestone pores, micromorphology, and mineral composition, with the degree of corrosion damage taken from the microscopic perspective. Li et al. [9], Lin et al. [10], and Zhang et al. [11] analyzed the influence of chemical corrosion on the porosity, pore structure, fracture process, deformation, and strength of limestone and sandstone samples from a micro–macro perspective, indicating that erosion from hydrochemical solution has a significant impact on the damage and failure of rocks. With the deepening of this research, it was found that in addition to the important influence of hydrochemical solution erosion on the damage and destruction of rocks, their mineral composition also has an important influence on the physical and mechanical properties of rocks [12–14], especially in terms of the process of hydrochemical solution erosion of rocks. The dissolution characteristics of mineral composition are varied, and the processes of rock erosion and destruction are jointly affected by the presence of a variety of mineral compositions [15–17].

China's acid rain area is one of the three largest acid rain areas in the world, after Europe and North America, and acid rain has covered 40% of the national territory. At present, southwest China is considered the region with the strongest acidity of its precipitation in the world, and the frequency of acid rain with a pH of <5.6 reaches 80%. The main acidogenic substances in precipitation are $SO_2{}^{-4}$ and $NO_3{}^{-}$, of which the concentration of $SO_2{}^{-4}$ is 5 to 10 times that of $NO_3{}^{-}$, which is much higher than the ratios in Europe, North America, and Japan. The precipitation is typical sulfuric acid rain. However, research on the damage and mechanical properties of rocks in an acid environment mostly focuses on hydrochloric acid and nitric acid solutions [5–7,9–11]. The Cl^{-} and $NO_3{}^{-}$ in these two forms combine with the Ca^{2+} precipitated in the rock to form water-soluble $CaCl_2$ or Ca $(NO_3)_2$. In a sulfuric acid solution, the $CaSO_4$ crystals generated by $SO_4{}^{2-}$ are not soluble in water, and the resulting microscopic damage to rock is different from that of hydrochloric acid and nitric acid solution. Therefore, it is necessary to study the microscopic damage characteristics of rock in a sulfuric acid solution.

In addition, limestone is an important building material and one of the most widely distributed minerals in the earth's crust. Its main component is calcium carbonate. The acidic environment has an obvious effect on the deterioration of limestone performance, which has been studied widely in the literature [18–24]. Based on this consideration, in this paper, limestone was soaked in a sulfuric acid solution for 5 days, 10 days, 15 days, and 20 days, respectively. The morphology, P-wave velocity, and wave velocity of acidic rock samples were analyzed using ultrasonic detection technology, scanning electron microscope technology, and energy spectrum analysis, and the micro damage phenomenon and mechanism of acidified limestone samples were studied.

2. Test Section

2.1. Test Sample Preparation

Each test sample is of limestone, and each sample is sourced from Yunnan, China. The sample size is a φ50 mm × 100 mm cylindrical specimen. Each sample has no obvious fissures and the maximum error of unevenness on both ends is not more than 0.05 mm. The discrete larger samples have previously been eliminated by the wave velocity test, as shown in Figure 1.

2.2. Test Methods and Apparatus

The samples were divided into five groups, and test groups 1 to 5 were subjected to an immersion time of 0, 5, 10, 15, and 20 days, respectively. All specimens were dried in an oven at 105 °C for 48 h before the test, and, after natural cooling, all specimens were placed in the immersion vessel. This container is cylindrical, with a diameter of 27 cm at the bottom and 30 cm at the top, and it is 38 cm in height. The volume of the sulfuric acid solution was 5 L, the concentration was 0.0158 mol/L, and the pH was 1.5.

Figure 1. Limestone specimen.

At the end of the immersion time for each group, first, the drying process was carried out, then the rock P-wave velocity measurements were carried out after natural cooling, and finally, the surface of the samples was examined by SEM. The selected equipment model for scanning electron microscope is a TESAN MAIA3LMU, the production place is in Brno, Czech, and the company is TESCAN Brnos.s.r.o. In addition, the detector type is SE. During the test, we placed the aluminum table with the sample on the support, the distance between the sample and the probe is 10 cm, and the acceleration voltage is 20 kV. The test procedure is shown in Figure 2. Step ①: dry the samples in the drying oven; step ②: conduct wave velocity and SEM tests on the dried samples; step ③: soak the samples in sulfuric acid solution for acidification after wave velocity and SEM tests; step ④: dry the samples after different acidification treatments and conduct wave velocity and SEM tests.

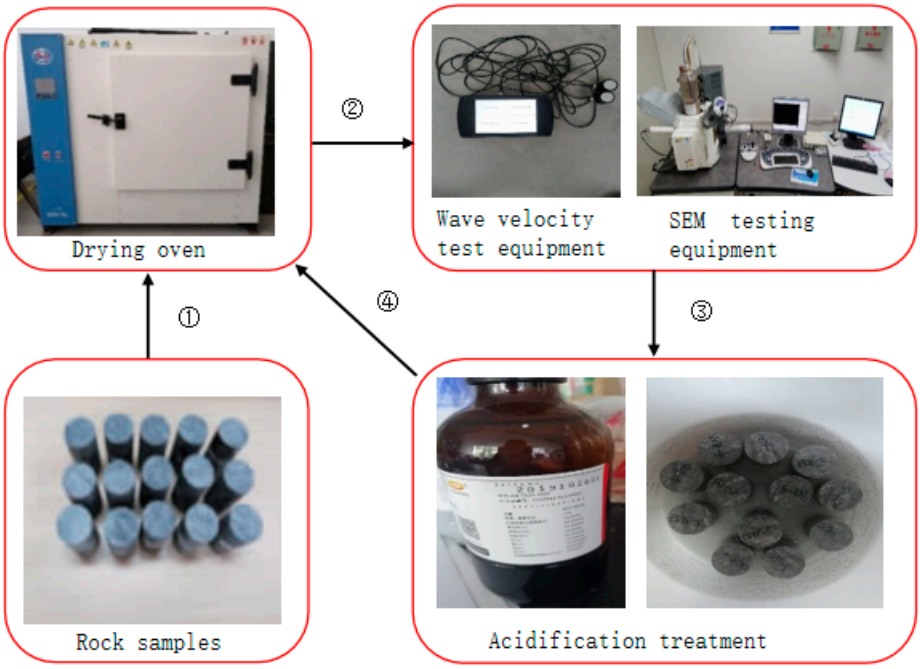

Figure 2. Test process.

3. Analysis of Morphological Changes in Appearance

Sulfuric acid is corrosive and can corrode rocks in a chemical reaction. Since the main component of limestone is calcium carbonate, sulfuric acid can react with calcium carbonate to form calcium sulfate. The surface morphology of each group of specimens is shown in Figure 3.

(**a**) Natural state (**b**) 5 days (**c**) 10 days (**d**) 15 days (**e**) 20 days

Figure 3. Limestone specimens after different soaking times under acidic conditions.

By observing the limestone samples soaked for different time periods under acidic conditions, the surface of the soaked sample appeared coarser. After soaking for 5 days, a thin protective film was formed on the surface of the sample. With the extension of soaking time, the protective film on the surface of the sample had a tendency to thicken. After soaking for 10 days, the surface of the sample showed large or small bumps. After soaking for 15 days, the bulge on the surface of the sample became more and more substantial; the whole rock sample surface was no longer smooth, and the surface roughness of the sample increased. After soaking for 20 days, the surface of the sample protruded and formed a large number of crystals attached to the surface after the accumulation in the early stage. The sample surface was analyzed via an energy spectrum, as shown in Figure 4. The ratio of S and Ca elements in the crystallite is 15.11% and 15.63%, respectively, and the value is close to 1:1. It is speculated that the crystallite generated on the sample surface is of $CaSO_4$.

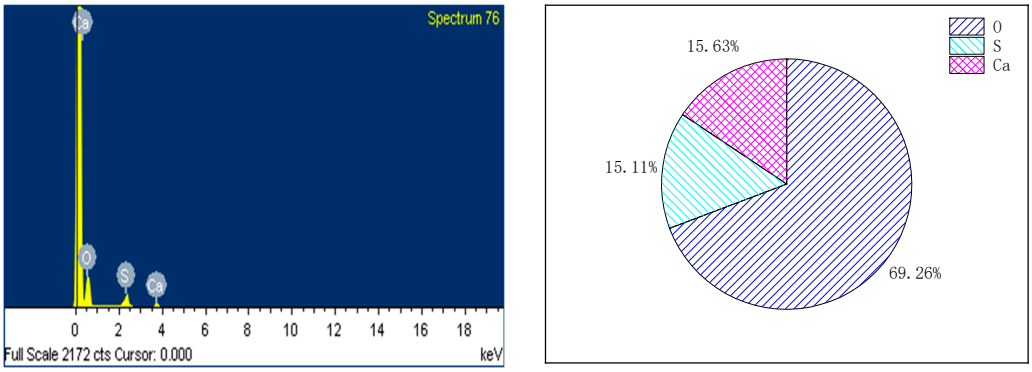

Figure 4. Results of the energy spectrum analysis of limestone specimens after immersion (20 days, concentration 0.0158 mol/L).

4. Wave Speed Test

4.1. P-Wave Velocity Analysis

Rock media ultrasonic technology is a non-destructive detection technique, based on the difference in wave velocity propagation speed in different media; the P-wave velocity can be used as a macroscopic characterization of the microstructure of the rock [25–27]. The P-wave velocities of the specimens are shown in Figure 5.

From Figure 6, the specimens showed a falling-rising-declining trend with increasing soaking time under acidic conditions; the change process was analyzed in 3 stages according to the law of change of their P-wave velocity with time.

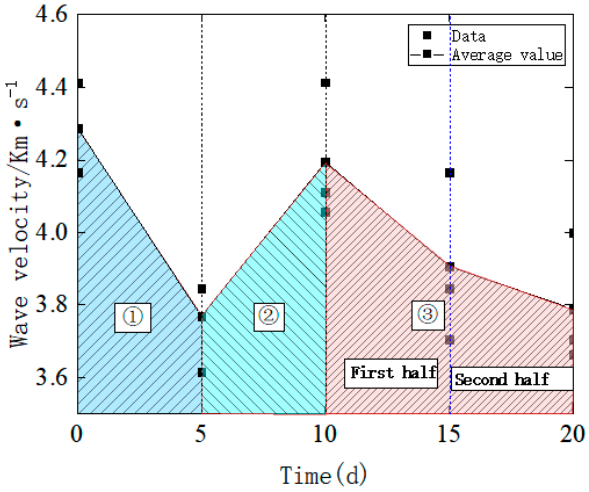

Figure 5. P-wave velocity variation curve.

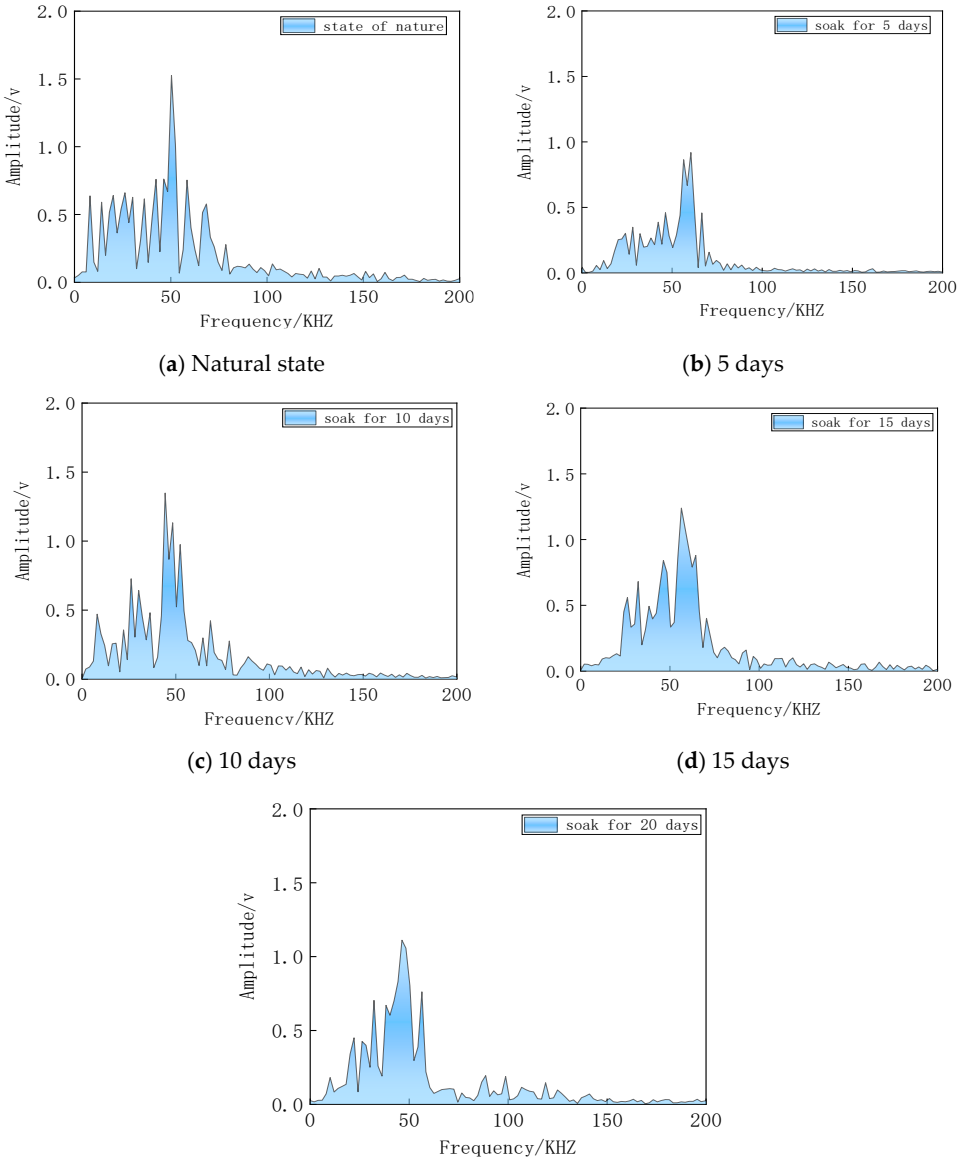

(**a**) Natural state

(**b**) 5 days

(**c**) 10 days

(**d**) 15 days

(**e**) 20 days

Figure 6. Spectrograms of acidified limestone samples after the different soaking times.

Phase (①) (falling stage): In the early stage of immersion, the hydration of the rock is mainly via chemical corrosion, due to the presence of a large amount of H+ in the strongly acidic solution, and the limestone specimens are dominated by calcite. Based on the results of the morphological analysis of the rock's appearance and the composition of the solution, the main reaction equation of its limestone chemical corrosion is presumed to be as follows:

$$2H^+ + CaCO_3 \rightarrow Ca^{2+} + CO_2\uparrow + H_2O$$

$$Ca^{2+} + SO_4{}^{2-} \rightarrow CaSO_4.$$

The chemical reaction between H+ and calcium carbonate in the limestone leads to damage to the internal structure, the further development of microcracks in the rock, the loosening of the internal structure, and the increase in porosity, which in turn shows the reduction of the rock P-wave velocity.

Phase (②) (rising stage): The wave velocity tends to rise, compared with the first stage. This is because, with the further corrosion of the acidic solution, the corrosion reaction zone gradually extends from the surface of the sample to the inside. However, due to the stress, water-insoluble calcium sulfate crystals will be produced, and the calcium sulfate crystals will stay in the internal cracks and fill in some of the internal microcracks, increasing the density of the rock, which will increase the wave velocity.

Phase (③) (descending phase): This phase can be subdivided into an upper half and a lower half.

In the first half, the P-wave velocity shows a decreasing trend, which is due to the water-absorbing quality of $CaSO_4$ crystals. As the immersion time increases, when the swelling effect of $CaSO_4$ crystals staying in the internal fissures due to water absorption is greater than the connection effect of the rock itself, it leads to the further expansion of the original fissures inside the rock and the sulphuric acid corrosion reaction zone will be further expanded inwards.

In the second half, the rock P-wave velocity continues to show a decreasing trend, but the decrease tends to be moderate. The analysis suggests that, firstly, as the chemical reaction continues, the amount of H+ in the solution decreases, which, together with the expansion of the corrosion reaction zone to the interior, causes the ion transport channels to become longer and the chemical reaction time to lengthen. Secondly, according to the analysis of the rock's appearance and morphological observations, a large number of crystalline substances were attached to the surface of the specimen; the presence of these crystals would prevent some of the H+ from entering the interior of the specimen for the chemical reaction, which to a certain extent would retard the damage to the specimen.

4.2. Acoustic Frequency Domain Signal Analysis

The information obtained by analyzing the P-wave velocities of rocks under different acidification conditions has some limitations, while the acoustic signals in the frequency domain contain a large amount of information about the internal structure of the rock. The waveform obtained in the wave velocity test was processed to obtain the frequency spectrum of the acoustic waves (see Figure 6), which shows that the acoustic signals in the frequency domain are mainly concentrated in the low-frequency region, with the absorption in the high-frequency part of the signals in the rock samples being more obvious. This is mainly due to the lower strength and pore structure of the limestone, the internal discontinuity is stronger, which is insensitive to the absorption of low-frequency signals and sensitive to the absorption and filtration of high-frequency signals [28].

For the amplitude of the main acoustic peak, the acoustic signal showed a certain regularity with the increase in soaking time, in which the rock samples showed a multi-peak phenomenon in the natural state, with an amplitude generally above 0.5 V and a high amplitude of the main peak (Figure 6a). After 5 days of soaking, the amplitude of the acoustic signal generally decreased, and the amplitude of the main peak decreased by 39.78%, compared with the natural state. After 10 days of immersion, the amplitude of the

acoustic signal improved, compared with that after 5 days of immersion, but it was still weaker than when in a natural state. Specifically, the amplitude of its main peak decreased by 11.67% compared with that in the natural state and increased by 46.68% compared with that after 5 days of immersion, and the signal showed enhanced oscillation. With the increase in soaking time, the amplitude of the acoustic signal dropped again. Compared with the natural state, the amplitude of the main peak after soaking for 15 days and 20 days decreased by 19.40% and 27.16%, respectively, as shown in Figure 7.

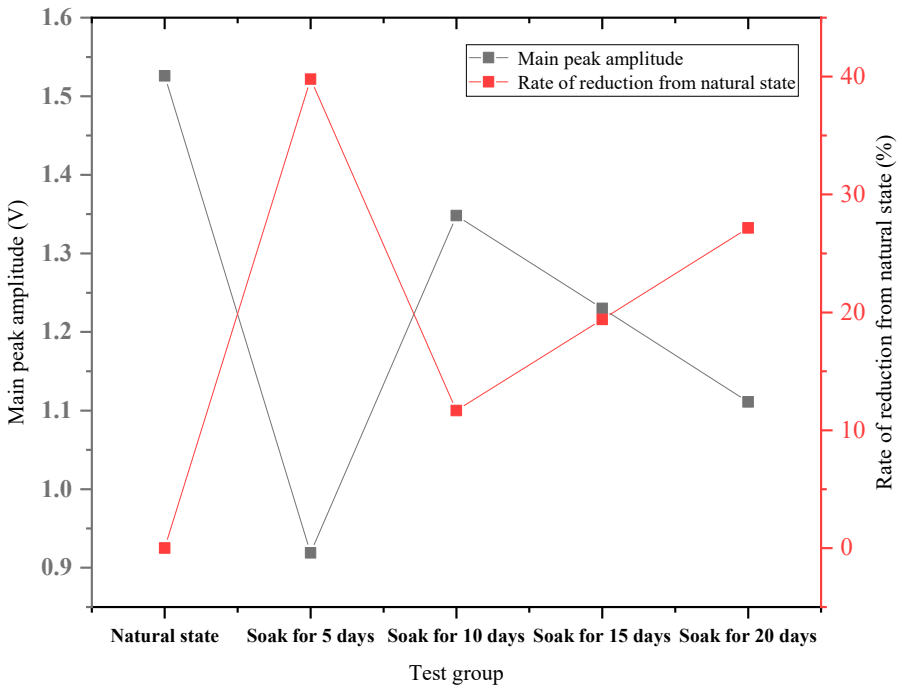

Figure 7. Characteristic values of the rock spectra after different soaking times under acidic conditions.

It is generally believed that the resistance slip between particles in dry rock samples will greatly affect the attenuation of sound waves. The main reason is that the inherent inelasticity of the medium and the friction loss caused by the relative movement between the particle interface and the crack surface will cause the attenuation of the main peak amplitude of the acoustic signal [28]. This is because the internal structure of the limestone sample is loose and the cracks develop due to the strong acid chemical reaction. The original cracks and secondary cracks are further expanded, resulting in an increase in the number of fracture surfaces in the rock, which leads to an increase in the number of relative movements between the internal particles and the fracture surface, and a corresponding increase in the number of friction movements. Finally, it shows that more energy is lost during the propagation of sound waves; the amplitude of the main peak of the acoustic signal weakens. However, because the $CaSO_4$ crystals filled part of the crack space in the middle period of immersion, the number of rock crack surfaces decreased compared with the initial period of immersion, resulting in relative movement between the internal particles and the crack surface. This showed that the amplitude of the main peak of the signal after immersion for 10 days was stronger than that after immersion for 5 days. It is clear that with an increase in soaking time, due to the water absorption and expansion of the $CaSO_4$ crystals, the cracks in the rock will open again, and the number of crack surfaces in the rock will rise again. With the increase in friction loss caused by the relative movement between particles and crack surfaces, the amplitude of the main peak of the signal will be weaker than that of the group soaked for 10 days.

5. Fractal Characteristics

The microstructure of rocks can often influence their macroscopic mechanical properties to a great extent; a number of studies have been carried out using SEM to investigate the structural morphology [29], porosity [30,31], and fractal dimensions [32,33] of rocks. Due to the anisotropic behavior of rocks, it is very difficult to study the geometric distribution and distribution laws of the pores. The research shows that the pore structure has fractal characteristics. The fractal dimension describes the irregularity of the material, i.e., the more disordered the material arrangement, the larger its fractal dimension, and conversely, the more homogeneous and neatly arranged the material, the smaller its fractal dimension. In this paper, an image with a magnification of 500 was obtained through SEM testing. On this basis, the fractal dimension of acidized rock pores was calculated using a box dimension algorithm. The grey-scale image obtained from the SEM was converted into a binary image, and the resulting image is shown in Figure 8.

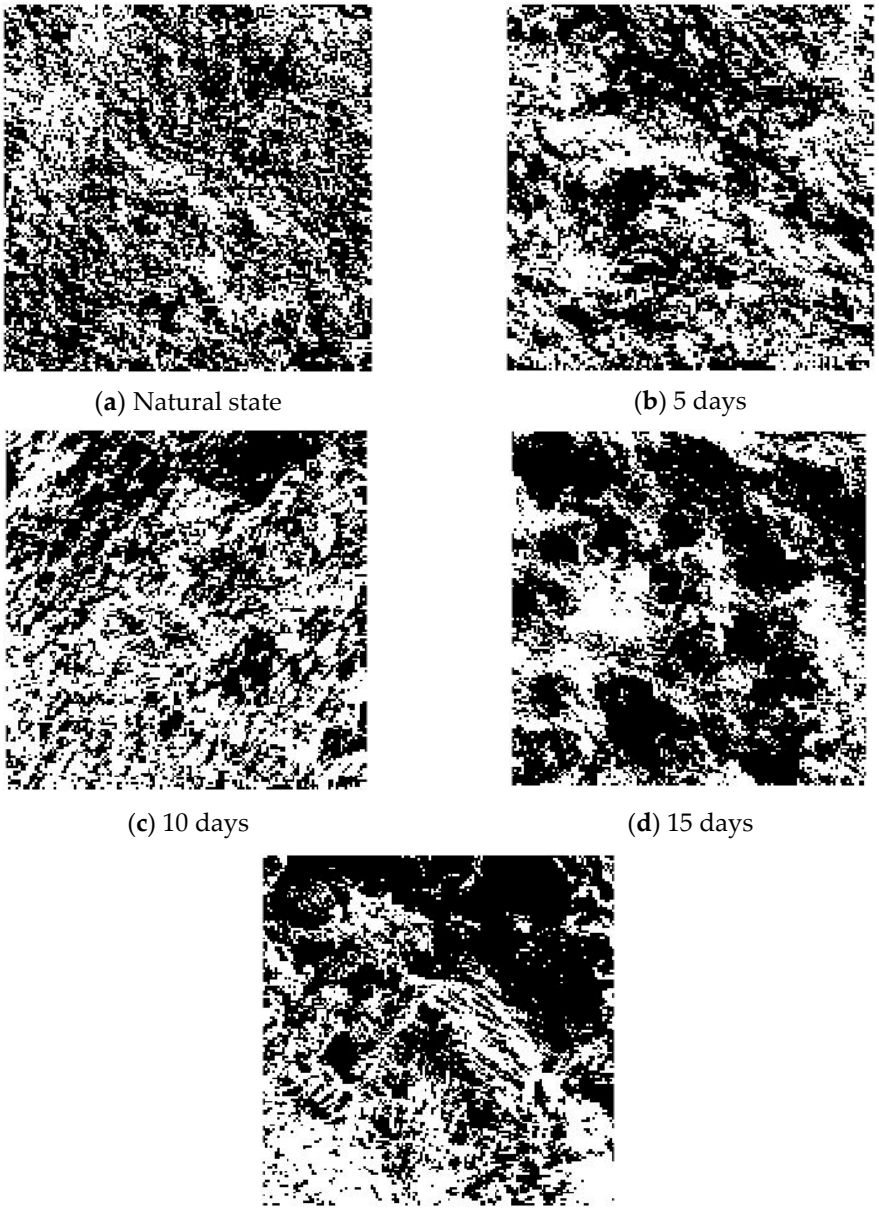

(**a**) Natural state (**b**) 5 days

(**c**) 10 days (**d**) 15 days

(**e**) 20 days

Figure 8. Binary images of rock samples under acidic conditions.

The fractal dimensions are calculated and obtained using the box-counting method. In this method, the image area is covered by a finite number of cubic boxes, the side length of which is ε. Then, by changing the side length of ε, the total number of cubic boxes $N(\varepsilon)$ can be varied. The relationship between $N(\varepsilon)$ and the side length ε can be expressed as follows [34]:

$$N(\varepsilon) \sim \varepsilon^{-D}.$$

After logarithmic transformation, a linear relationship between $\ln N(\varepsilon)$ and $\ln\varepsilon$ is obtained. Then, the surface fractal dimension D in the boxcounting method can be calculated as follows:

$$D = -\lim_{\varepsilon \to 0} \frac{\ln N(\varepsilon)}{\ln \varepsilon} \quad (1)$$

The representative calculation results of the fractal dimension are shown in Figure 9, where the slope of the curve is the fractal dimension.

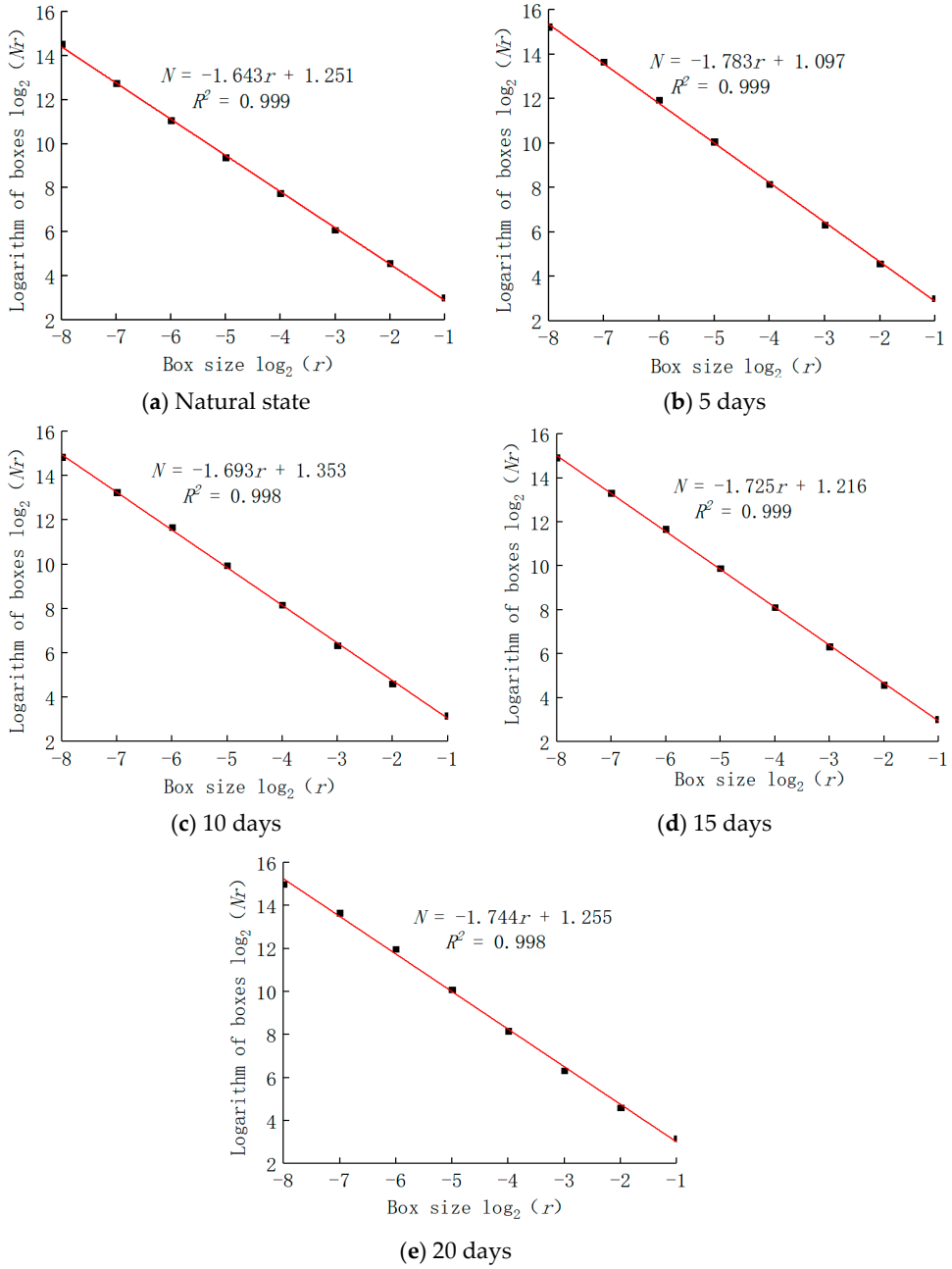

Figure 9. Fractal dimension under different acidification time.

For a more concise representation of the fractal dimension at different acidification times, please see Figure 10. The average value of the fractal dimension under different soaking times is 1.64, 1.79, 1.69, 1.72, and 1.65, respectively. It can be seen that the fractal dimension generally increases during the immersion period. In each time period, the fractal dimension first increases, then decreases, and then increases again with increasing immersion time. This shows that the $CaSO_4$ crystals filled in some fractal spaces on the surface of the rock samples during immersion, which increased the density of the rocks to a certain extent.

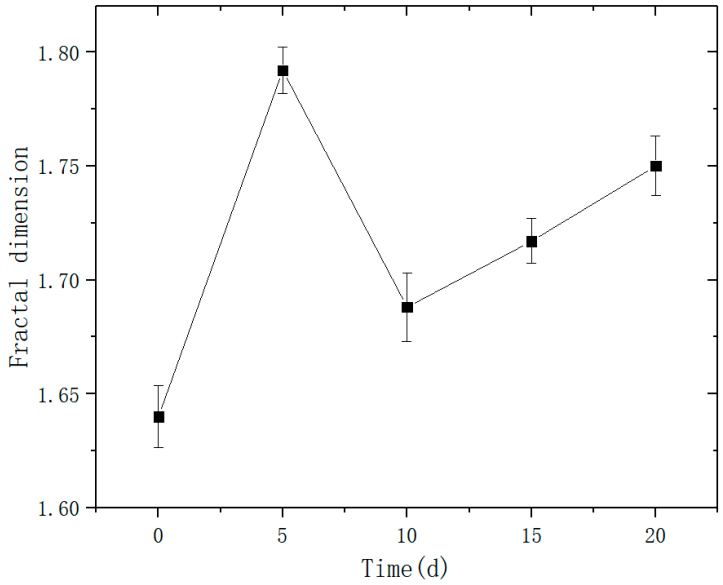

Figure 10. The fractal dimension of the limestone under acidic conditions.

6. Conclusions

In this paper, the limestone samples are soaked in sulfuric acid. Through an analysis of the apparent phenomenon seen in the samples, the wave velocity of the samples has been measured with an ultrasonic tester. At the same time, the changes in the mesostructure of limestone samples in an acid environment were studied using fractal theory, with the help of SEM. The main conclusions are as follows:

(1) The analysis of limestone acidification in the sulfuric acid solution environment shows that the internal damage to rock increases as a whole in the sulfuric acid solution immersion environment; however, this is not a single linear trend, and the damage decreases after a certain period of time. This is because the sulfuric acid solution immersion will produce calcium sulfate crystals in the micro cracks, filling part of the internal crack space, and will reduce the damage degree in this period.

(2) Through the analysis of acoustic time-domain signal and frequency-domain signal, the results show that the rock-wave velocity in the time-domain state is degraded to varying degrees, compared with the natural state; the acoustic signal has an obvious absorption effect on high frequency, and the variation trend of the main peak amplitude with the soaking time is consistent.

(3) The pore distribution of a limestone mesostructure under acidic conditions has fractal characteristics; the fractal dimension D first increases, then decreases, and then increases with the increase in soaking time.

Author Contributions: Conceptualization, C.L. and X.C.; methodology, X.C.; software, X.L. and L.L.; validation, X.C., C.L. and X.L.; formal analysis, H.L.; investigation, X.L.; resources, X.C.; writing—X.L. and H.L.; writing—review and editing, C.L. All authors have read and agreed to the published version of the manuscript.

Funding: This work is financially supported by the open project of the National Natural Science Foundation of China (52204156; 51904248), and the Sichuan Natural Science Foundation (2022NSFSC1147), the Shock and Vibration of Engineering Materials and Structures Key Laboratory of Sichuan Province (20kfgk07).

Institutional Review Board Statement: Not applicable.

Informed Consent Statement: Not applicable.

Data Availability Statement: No new data were created or analyzed in this study. Data sharing was not applicable to this study.

Acknowledgments: The authors appreciate the anonymous reviewers for their constructive comments and suggestions that significantly improved the quality of this manuscript.

Conflicts of Interest: The authors declare no conflict of interest.

References

1. Zhao, Z.H.; Yang, J.; Zhang, D.F.; Peng, H. Effects of wetting and cyclic wetting–drying on tensile strength of sandstone with a low clay mineral content. *Rock Mech. Rock Eng.* **2017**, *50*, 485–491. [CrossRef]
2. Zhou, Z.L.; Cai, X.; Ma, D.; Chen, L.; Wang, S.; Tan, L. Dynamic tensile properties of sandstone subjected to wetting and drying cycles. *Constr. Build. Mater.* **2018**, *182*, 215–232. [CrossRef]
3. Zhang, Z.Z.; Niu, Y.X.; Shang, X.J.; Ye, P.; Zhou, R.; Gao, F. Deterioration of physical and mechanical properties of rocks by cyclic drying and wetting. *Geofluids* **2021**, *2021*, 6661107. [CrossRef]
4. Li, X.; Liu, Z.; Feng, X.; Zhang, H.; Feng, J. Effects of Acid Sulfate and Chloride Ion on the Pore Structure and Mechanical Properties of Sandstone Under Dynamic Loading. *Rock Mech. Rock Eng.* **2021**, *54*, 6105–6121. [CrossRef]
5. Tong, R.; Liu, H.; Liu, J.; Shi, Y.; Xie, L.; Ban, S. Meso-Mechanical Characteristics of Granite with Natural Cracks after Mud Acid Corrosion. *Energies* **2022**, *15*, 721. [CrossRef]
6. Morsy, S.; Hetherington, C.; Sheng, J. Effect of low-concentration HCl on the mineralogy, physical and mechanical properties, and recovery factors of some shales. *J. Unconv. Oil Gas Resour.* **2015**, *9*, 94–102. [CrossRef]
7. Feng, X.T.; Chen, S.L.; Li, S.J. Effects of water chemistry on microcracking and compressive strength of granite. *Int. J. Rock Mech. Min. Sci.* **2001**, *38*, 557–568. [CrossRef]
8. Yu, L.Y.; Zhang, Z.Q.; Wu, J.Y.; Liu, R.; Qin, H.; Fan, P. Experimental study on the dynamic fracture mechanical properties of limestone after chemical corrosion. *Theor. Appl. Fract. Mech.* **2020**, *108*, 102620. [CrossRef]
9. Li, H.; Zhong, Z.L.; Liu, X.R.; Sheng, Y.; Yang, D. Micro-damage evolution and macro-mechanical property degradation of limestone due to chemical effects. *Int. J. Rock Mech. Min. Sci.* **2018**, *110*, 257–265. [CrossRef]
10. Lin, Y.; Zhou, K.P.; Gao, R.G.; Li, J.; Zhang, J. Influence of chemical corrosion on pore structure and mechanical properties of sandstone. *Geofluids* **2019**, *2019*, 7320536. [CrossRef]
11. Zhang, J.; Deng, H.; Taheri, A.; Ke, B.; Liu, C.; Yang, X. Degradation of physical and mechanical properties of sandstone subjected to freeze-thaw cycles and chemical erosion. *Cold Reg. Sci. Technol.* **2018**, *155*, 37–46. [CrossRef]
12. Li, H.M.; Li, H.G.; Wang, K.L.; Liu, C. Effect of rock composition microstructure and pore characteristics on its rock mechanics properties. *Int. J. Min. Sci. Technol.* **2018**, *28*, 303–308. [CrossRef]
13. Li, Q.; Li, J.P.; Duan, L.C.; Tan, S. Prediction of rock abrasivity and hardness from mineral composition. *Int. J. Rock Mech. Min. Sci.* **2021**, *140*, 104658. [CrossRef]
14. Zhang, W.Q.; LU, C. Effects of mineral content on limestone properties with exposure to different temperatures. *J. Pet. Sci. Eng.* **2020**, *188*, 106941. [CrossRef]
15. Liu, Y.Q.; Sun, C.; Xiong, Y.; Wu, W.; Zhang, Y.; Li, N. Kinetics study of surface reaction between acid and sandstone based on the rotation disk instrument. *Chem. Technol. Fuels Oils* **2020**, *55*, 765–777. [CrossRef]
16. Marieni, C.; Matter, J.M.; Teagle, D.A.H. Experimental study on mafic rock dissolution rates within CO_2-Sea water rock systems. *Geochim. Et Cosmochim. Acta* **2020**, *272*, 259–275. [CrossRef]
17. Ivanishin, I.B.; Nasr-El-din, H.A. Effect of calcium content on the dissolution rate of Dolomites in HCl acid. *J. Pet. Sci. Eng.* **2021**, *202*, 108463. [CrossRef]
18. Zhang, Y.; Wang, Z.; Su, G.S.; Wu, Z.K.; Liu, F.T. Experimental Investigation on Influence of Acidic Dry-Wet Cycles on Karst Limestone Deterioration and Damage. *Geofluids* **2022**, *2022*, 8562226. [CrossRef]
19. Lai, J.; Guo, J.C.; Ma, Y.X.; Zhou, H.Y.; Wang, S.B.; Liu, Y.X. Effect of Acid-Rock Reaction on the Microstructure and Mechanical Property of Tight Limestone. *Rock Mech. Rock Eng.* **2022**, *55*, 35–49. [CrossRef]
20. Ding, W.X.; Wang, H.Y.; Chen, H.J.; Ma, T. Mechanical Damage and Chemical Dissolution Kinetic Features of Limestone under Coupled Mechanical-Hydrological-Chemical Effects. *Geofluids* **2021**, *2021*, 1810768. [CrossRef]
21. Niazi, F.S.; Piñán-Llamas, A.; Fekadu, F. Impact of chemical weathering on microstructures and mechanical properties of karstic limestone. *Geotech. Lett.* **2021**, *11*, 281–293. [CrossRef]

22. Li, H.; Zhong, Z.L.; Eshiet, K.I.-I.; Sheng, Y.; Liu, X.R.; Yang, D. Experimental Investigation of the Permeability and Mechanical Behaviours of Chemically Corroded Limestone Under Different Unloading Conditions. *Rock Mech. Rock Eng.* **2020**, *53*, 1587–1603. [CrossRef]
23. Scrivano, S.; Gaggero, L. An experimental investigation into the salt-weathering susceptibility of building limestones. *Rock Mech. Rock Eng.* **2020**, *53*, 5329–5343. [CrossRef]
24. Yao, H.; Ma, D.; Xiong, J. Study on the Influence of Different Aqueous Solutions on the Mechanical Properties and Microstructure of Limestone. *J. Test. Eval.* **2020**, *49*, 3776–3794. [CrossRef]
25. Zhang, Y.; Wu, W.; Yao, X.; Liang, P.; Sun, L.; Liu, X. Study on Spectrum Characteristics and Clustering of Acoustic Emission Signals from Rock Fracture. *Circuits Syst. Signal Process.* **2020**, *39*, 1133–1145. [CrossRef]
26. Wu, S.; Qin, G.; Cao, J. Deformation, Failure, and Acoustic Emission Characteristics under Different Lithological Confining Pressures. *Materials* **2022**, *15*, 4257. [CrossRef]
27. Du, K.; Li, X.; Tao, M.; Wang, S. Experimental study on acoustic emission (AE) characteristics and crack classification during rock fracture in several basic lab tests. *Int. J. Rock Mech. Min. Sci.* **2020**, *133*, 104411. [CrossRef]
28. Zhang, M.M.; Liang, L.X.; Jiang, S.L. Influence of carbonate rocks with different pore structures on the time-frequency characteristics of acoustic waves. *Broken Block Oil Gas Field* **2016**, *23*, 825–828.
29. Ersoy, H.; Atalar, C.; Sünnetci, M.O.; Kolaylı, H.; Karahan, M.; Ersoy, A.F. Assessment of damage on geo-mechanical and micro-structural properties of weak calcareous rocks exposed to fires using thermal treatment coefficient. *Eng. Geol.* **2021**, *284*, 106046. [CrossRef]
30. Hu, Z.; Lu, S.; Klaver, J.; Dewanckele, J.; Amann-Hildenbrand, A.; Gaus, G.; Littke, R. An Integrated Imaging Study of the Pore Structure of the Cobourg Limestone—A Potential Nuclear Waste Host Rock in Canada. *Minerals* **2021**, *11*, 1042. [CrossRef]
31. Wu, X.; Guo, Q.; Zhu, Y.; Ren, F.; Zhang, J.; Wu, X.; Cai, M. Pore structure and crack characteristics in high-temperature granite under water-cooling. *Case Stud. Therm. Eng.* **2021**, *28*, 101646. [CrossRef]
32. Li, X.; Wei, W.; Wang, L.; Ding, P.; Zhu, L.; Cai, J. A new method for evaluating the pore structure complexity of digital rocks based on the relative value of fractal dimension. *Mar. Pet. Geol.* **2022**, *141*, 105694. [CrossRef]
33. Huang, D.; Chang, X.; Tan, Y.; Fang, K.; Yin, Y. From rock microstructure to macromechanical properties based on fractal dimensions. *Adv. Mech. Eng.* **2019**, *11*, 168781401983636. [CrossRef]
34. Cao, R.H.; Wang, C.S.; Yao, R.B.; Hu, T.; Lei, D.X.; Lin, H.; Zhao, Y.L. Effects of cyclic freeze-thaw treatments on the fracture characteristics of sandstone under different fracture modes: Laboratory testing. *Theor. Appl. Fract. Mech.* **2020**, *109*, 102738. [CrossRef]